

Astrophysical constraints on hypothetical variability of fundamental constants

Sergei A. Levshakov

Department of Theoretical Astrophysics, Ioffe Physico-Technical Institute,
Politekhnicheskaya Str. 26, 194021 St. Petersburg, Russia

Abstract

Many-multiplet (MM) method [1] applied to Keck/HIRES quasar absorption spectra gives a shift in the value of the fine-structure constant of $\Delta\alpha/\alpha = (-5.4 \pm 1.2) \times 10^{-6}$ [2]. Theoretical models of the fundamental physical interactions predict in this case a shift in the proton-to-electron mass ratio ($\mu = m_p/m_e$) of about $\Delta\mu/\mu \sim -2 \times 10^{-4}$. We used VLT/UVES high-resolution observations of molecular hydrogen H₂ ultraviolet absorption lines to test this prediction and found that at redshift $z = 3.025$ $\Delta\mu/\mu = (2.1 \pm 3.6) \times 10^{-5}$. We also present a modified MM method to set an upper limit on $\Delta\alpha/\alpha$ from a homogeneous sample of Fe II lines identified in the up-to-date best quality VLT/UVES spectrum of HE 0515–4414. Our result is $\Delta\alpha/\alpha = (1.1 \pm 1.1) \times 10^{-5}$ at redshift $z = 1.149$. Future observations with a new High Accuracy Radial velocity Planet Searcher (HARPS) spectrograph may provide a crucial test for the $\Delta\alpha/\alpha$ measurements at a level of 10^{-6} .

1 Introduction

The purpose of this paper is to outline some problems related to the measurements of the dimensionless fundamental constants from quasar (QSO) absorption-line spectra: the fine-structure constant $\alpha = e^2/\hbar c$ and the proton-to-electron mass ratio $\mu = m_p/m_e$, which characterize the strength of electromagnetic and strong interactions, respectively.

The current interest in this field stems from the prospect of using the high-resolution spectra of extragalactic objects to measure with high accuracy the transition energies of a certain ionic species and molecules at different cosmological redshifts z^1 . If physical constants varied in the past, then the comparison of the transition energies measured from QSO spectra with their laboratory values provides direct astrophysical constraints on the ratios α_z/α and μ_z/μ over a cosmological time-scale ($\Delta t \sim 10^{10}$ yr). We define $\Delta\alpha/\alpha = (\alpha_z - \alpha)/\alpha$ and $\Delta\mu/\mu = (\mu_z - \mu)/\mu$, where index z marks the values of the fine-structure constant and the proton-to-electron mass ratio at redshift z , whereas their laboratory values at $z = 0$ are denoted by α and μ , respectively². At present, these constants are measured with the relative accuracies $\delta_\alpha = 4 \times 10^{-9}$ and $\delta_\mu = 2 \times 10^{-9}$ and their values are equal to $\alpha = 1/137.03599958$ and $\mu = 1836.1526670$ [3].

The variability of the fundamental constants was firstly suggested by Milne [4] and Dirac [5] who assumed that the Newtonian gravitational constant G may change in cosmic time. Different functional forms for the time variations of G and other constants were later considered in a series of publications (see [6], for a review). The variability of α caused by a coupling between electromagnetism and gravity is considered within the framework of different modifications of the Kaluza-Klein theory (e.g., [7]-[12]). The number of theoretical publications on this topic is considerably increased in the last two years.

For astronomical observations, it is more convenient to deal with dimensionless constants since they are independent on the choice of physical units. That is why most efforts to reveal hypothetical variability of constants are connected with measurements of α (see [2, 13] and references cited therein).

First observational study (1967) of the time dependence of α from QSO absorption spectra was based on the analysis of alkali doublets (AD method) and yielded $\Delta\alpha/\alpha = -0.02 \pm 0.05$ at $z = 1.95$ [14]. Since then, there have been made many other AD studies of $\Delta\alpha/\alpha$ with increasing accuracy in accord with increasing quality of observations: $\Delta\alpha/\alpha = (0 \pm 1.5) \times 10^{-3}$ at $z = 3.2$ [15], $\Delta\alpha/\alpha = (-4.5 \pm 4.3 \pm 1.4) \times 10^{-5}$ at $z = 2 - 4$ [16], $\Delta\alpha/\alpha = (-0.5 \pm 1.3) \times 10^{-5}$ at $z = 2 - 3$ [17]. However, the use of absorption lines

¹ $z = (\lambda - \lambda_0)/\lambda_0$, where λ is the observed wavelength of a given ionic transition and λ_0 is the corresponding rest frame (laboratory) value. Modern observational data are ranging from $z = 0$ (the Milky Way) up to $z \sim 6$ (distant QSOs).

²In the literature μ is sometimes referred to its inverse value, $\mu^* = m_e/m_p$. In this case $\Delta\mu^*/\mu^* = -\Delta\mu/\mu$.

from different multiplets in different ions, the so-called many-multiplet (MM) method, may in principle increase the accuracy of these $\Delta\alpha/\alpha$ estimations [1, 2].

Applying the MM method to three samples of Keck/HIRES QSO data, Murphy et al. [2] obtained a statistically significant negative value of $\Delta\alpha/\alpha = (-5.4 \pm 1.2) \times 10^{-6}$ in the redshift interval $0.2 < z < 3.7$. In spite of all advantages of the MM method, the result is nevertheless surprising since it implicitly assumes extremely stable conditions during the observing nights and unrealistically homogeneous physical parameters in the absorption clouds. We consider computational caveats of the AD and MM methods in Section 2.

If α is supposed to be time dependent, the other gauge coupling constants should also depend on time as predicted by theoretical models of the fundamental physical interactions. For instance, within the framework of a unified theory (e.g., supersymmetric SU(5)) the time variation of α at low energies is caused by a time variation of the unification scale Λ ($= 213^{+38}_{-35}$ MeV), which, in turn, leads to a time variation of the proton mass m_p :

$$\frac{\Delta m_p}{m_p} = \frac{\Delta \Lambda}{\Lambda} = \mathcal{R} \frac{\Delta \alpha}{\alpha}, \quad (1)$$

where the numerical coefficient \mathcal{R} ($\simeq 40$) is known with an uncertainty of about 20% [18].

Assuming that the possible time changes of the electron mass or the quarks masses are negligible, the relation (1) suggests that a variation of $\Delta\alpha/\alpha \simeq -5.4 \times 10^{-6}$ should be accompanied by a shift in the proton-to-electron mass ratio of $\Delta\mu/\mu \sim -2 \times 10^{-4}$. This prediction can be tested by measuring the electronic-vibrational-rotational lines of the H_2 molecule observed in QSO spectra at high- z as described in [19]. We discuss this test in Section 3. Our conclusions and remarks for future prospects are summarized in Section 4.

2 Methods to constrain $\Delta\alpha/\alpha$ from QSO absorption spectra

2.1 The alkali-doublet (AD) method

The value of the fine-structure constant α_z at redshift z can be directly estimated from the relative wavelength separation between the fine-splitting

lines of an alkali doublet (AD method) [20]:

$$\frac{\alpha_z}{\alpha} = \left(\frac{\Delta\lambda_z}{\langle\lambda\rangle_z} \right) \left(\frac{\Delta\lambda}{\langle\lambda\rangle} \right)^{1/2}, \quad (2)$$

where $\Delta\lambda_z$ and $\langle\lambda\rangle_z$ are, respectively, the fine-structure separation and the weighted mean wavelength for a given doublet from a QSO absorption system at redshift z , while $\Delta\lambda$ and $\langle\lambda\rangle$ denote the same quantities from laboratory data.

The uncertainty $\sigma_{\Delta\alpha/\alpha}$ in the individual measurement can be estimated from [21]:

$$\sigma_{\Delta\alpha/\alpha} \simeq \frac{1}{\sqrt{2}} \left(\delta_{\lambda_z}^2 + \delta_{\lambda}^2 \right)^{1/2}, \quad (3)$$

where $\delta_{\lambda_z} = \sigma_{\lambda_z}/\Delta\lambda_z$, $\delta_{\lambda} = \sigma_{\lambda}/\Delta\lambda$, and σ_{λ_z} , σ_{λ} are, respectively, the errors of the wavelengths in the absorption system and laboratory.

Equation (2) shows that the AD method uses only the wavelength ratios and thus it does not require the measurements of absolute wavelengths. This fact excludes large systematic errors caused by the wavelength calibration in a wide spectral range. Therefore the accuracy of the AD measurements is mainly restricted by statistical fluctuations in the recorded counts at different wavelengths within the line profile.

The measurement of the line profile parameters and their errors are thoroughly described in [22]. The midpoint λ_c of an interval over M pixels covering the line profile can be calculated from the equations

$$\lambda_c = \frac{a}{W_{\lambda}} \sum_{i=1}^M \lambda_i (1 - I_i/C_i), \quad (4)$$

and

$$W_{\lambda} = a \sum_{i=1}^M (1 - I_i/C_i), \quad (5)$$

where W_{λ} is the equivalent width, a is the wavelength interval between pixels, I_i is the observed count rate at pixel i , C_i is the continuum count rate at pixel i , and λ_i is the wavelength at pixel i .

The errors in λ_c and W_{λ} caused by counting statistic and the uncertainty of the overall height of the continuum level are given by [22]:

$$\sigma_{\lambda_c} = \frac{a}{W_{\lambda}} \left[\left\langle \frac{\sigma_I}{C} \right\rangle^2 (A - 2\lambda_c B + M\lambda_c^2) + \left\langle \frac{\sigma_C}{C} \right\rangle^2 (B - M\lambda_c)^2 \right]^{1/2}, \quad (6)$$

and

$$\sigma_{W_\lambda} = a \left[\langle \sigma_I/C \rangle^2 M + \langle \sigma_C/C \rangle^2 (M - W_\lambda/a)^2 \right]^{1/2}, \quad (7)$$

where $A = \sum_i \lambda_i^2$, $B = \sum_i \lambda_i$, $\langle \sigma_I/C \rangle$ is the inverse mean signal-to-noise (S/N) $^{-1}$ ratio over the line measurement interval, and $\langle \sigma_C/C \rangle$ is the mean accuracy of the continuum level.

If the rms error of the wavelength scale calibration is σ_{sys} , then the total error is given by the sum

$$\sigma_{\text{tot}}^2 = \sigma_{\lambda_c}^2 + \sigma_{\text{sys}}^2. \quad (8)$$

The error of the wavelength scale calibration is related to the radial velocity accuracy as

$$\sigma_v = c \sigma_{\text{sys}} / \lambda, \quad (9)$$

where c is the speed of light.

For example, $\sigma_{\text{sys}} \simeq 0.002 \text{ \AA}$ for VLT/UVES data [23] corresponds at 5000 \AA to $\sigma_{\text{sys}} = 0.12 \text{ km s}^{-1}$. If $\sigma_{\lambda_c} = 0.002 \text{ \AA}$, then for the Mg II $\lambda\lambda 2796, 2803 \text{ \AA}$ doublet (3) gives $\sigma_{\Delta\alpha/\alpha} = 1.3 \times 10^{-4}$ at $z = 2$, which is a typical accuracy for the individual AD estimations from isolated doublets with $W_\lambda \sim 100 \text{ m\AA}$. Equation (6) shows that σ_{λ_c} decreases linearly with W_λ , meaning that, not surprisingly, the error for weak absorption lines ($W_\lambda \ll 1 \text{ \AA}$) may be very large. For example, the rest-frame equivalent widths for Fe II $\lambda 1608 \text{ \AA}$ and $\lambda 1611 \text{ \AA}$ at $z = 3.39$ toward Q0000–2620 measured from the Keck/HIRES data are $W_{1608} \simeq 0.178 \text{ \AA}$ and $W_{1611} \simeq 0.003 \text{ \AA}$ [24], i.e. the measured errors σ_{λ_c} for these lines should differ by ~ 50 times. It is clear that to achieve the highest accuracy in the $\Delta\alpha/\alpha$ estimations by means of the the AD method only well separated and unsaturated doublets with $W_\lambda \sim 100 \text{ m\AA}$ should be selected for the analysis.

2.2 The many-multiplet (MM) method

The many-multiplet (MM) method is a generalization of the AD method (see [2] and references therein). The method uses many transitions from different multiplets and different ions observed in a QSO absorption system. The line profiles selected for the MM analysis are represented by a sum of the same number of components (Voigt profiles) each of which is defined by three individual parameters (the column density, the Doppler width or

b -parameter, and the redshift z_i) and a common value of $\Delta\alpha/\alpha$. The rest wavenumbers in the MM method can be altered according to [2]

$$\omega_z = \omega_0 + q x_z , \quad (10)$$

where

$$x_z = (\alpha_z/\alpha)^2 - 1 , \quad (11)$$

and ω_z , ω_0 are the rest-frame wavenumbers of a transition in a QSO system with redshift z and measured in the laboratory, respectively. The sensitivity coefficients q (determining the sensitivity of ω_0 to the variation of α) are listed in Table 2 in [2].

All parameters are estimated through the minimization of χ^2 simultaneously for the whole set of lines. A significant improvement in the accuracy of the $\Delta\alpha/\alpha$ estimations by the MM method compared to the AD method is due to a wide range of the q values (see Section 2.3 below). Nevertheless, the MM method has some immanent shortcomings which could affect the claimed accuracy $\sigma_{\langle\Delta\alpha/\alpha\rangle} = 1.2 \times 10^{-6}$.

First of all, the weakest point of the MM method is the multiple velocity component Voigt profile deconvolution. From mathematical point of view, any deconvolution itself is a typical *ill-posed* problem [25]. When several smoothing operators (like convolution with the spectrograph point-spread function, summing, and integrating) are involved in the minimization procedure, the ill-posing may cause quite ambiguous results. In case of complex line profiles when many components are required to describe the whole profile, the fitting parameters cannot be estimated with high accuracy because of strong *inter-parameter correlations*. For example, the value of $\Delta\alpha/\alpha$ can be artificially constrained by the increase of the component number or by variations of b -values. Thus, to enhance the reliability of the results only simple line profiles (requiring minimum number of components) should be taken into MM analysis.

From physical point of view, the Voigt profile deconvolution assumes that the complex profile is caused by separate clouds lined along the line of sight with different radial velocities, each having its own constant gas density, kinetic temperature and, hence, its own ionization state. However, observations of QSOs have shown that with increasing spectral resolution more and more subcomponents appear in the line profile. This complexity indicates that, in general, metal lines arise in continuous turbulent media with fluctuating velocity and density fields.

We note in passing that the highest spectral resolution achieved in observations of QSOs at modern giant telescopes is $\sim 5 \text{ km s}^{-1}$ ($FWHM$), whereas the expected values for minimum (thermal) widths of metal lines are less or about 1 km s^{-1} for typical kinetic temperatures $100 \text{ K} < T_{\text{kin}} < 10^4 \text{ K}$. This means that we are still not able to measure directly the true intensity in the line profile but observe only the apparent intensity which is a convolution of the true spectrum and the spectrograph point-spread function.

Thus, to measure the transition energies, the distribution function of the radial velocities within the intervening cloud must be known for the AD method, whereas the MM method requires in addition the knowledge of the density distribution, for it deals with ions of different elements which may not arise co-spatially [26]. Since the velocity and density distributions are determined from the same line profiles which are used in the measurements of $\Delta\alpha/\alpha$, it is not possible to discriminate among kinematic effects and possible changes in α on the basis of only one absorption system. But if we have many absorption systems, statistical approach may probably solve this problem if shifts in the measured $\Delta\alpha/\alpha$ values are of random nature and, thus, can be averaged out in a large ensemble of absorption systems where any deviations in velocity distributions of different ions are equally probable.

Shifts in $\Delta\alpha/\alpha$ may also arise if the main assumption of the MM method that different ionic species trace exactly each other in their space distribution is not adequate. Dissimilarities in the line profiles of different ions may be caused by density fluctuations leading to inhomogeneous photoionization in the absorption cloud.

The QSO absorption clouds is a very inhomogeneous population. Their linear sizes, L , can be estimated from the observed neutral hydrogen column densities, $N(\text{H I}) \sim 10^{20} - 10^{21} \text{ cm}^{-2}$, and the estimated gas number densities, $n_{\text{H}} \sim 10^{-2} - 1 \text{ cm}^{-3}$, giving $L = N(\text{H I})/n_{\text{H}} \sim 10\text{s pc} - 10\text{s kpc}$. The intervening clouds may also contain small dense filaments with much higher densities ($n_{\text{H}} \sim 10^2 \text{ cm}^{-3}$) and the line-of-sight sizes less than 1 pc [27].

It is usually assumed that the metal absorbers in QSO spectra are in photoionization equilibrium with the ambient metagalactic UV background. To describe the thermal and the ionization state of the gas in the diffuse clouds it is convenient to introduce the dimensionless ‘ionization parameter’ $U = n_{\text{ph}}/n_{\text{H}}$, equal to the ratio of the number of photons in 1 cm^3 with energies above one Rydberg to the gas number density.

For illustrative purpose, we will assume that the UV background is not time or space dependent and that its shape and intensity is given by the

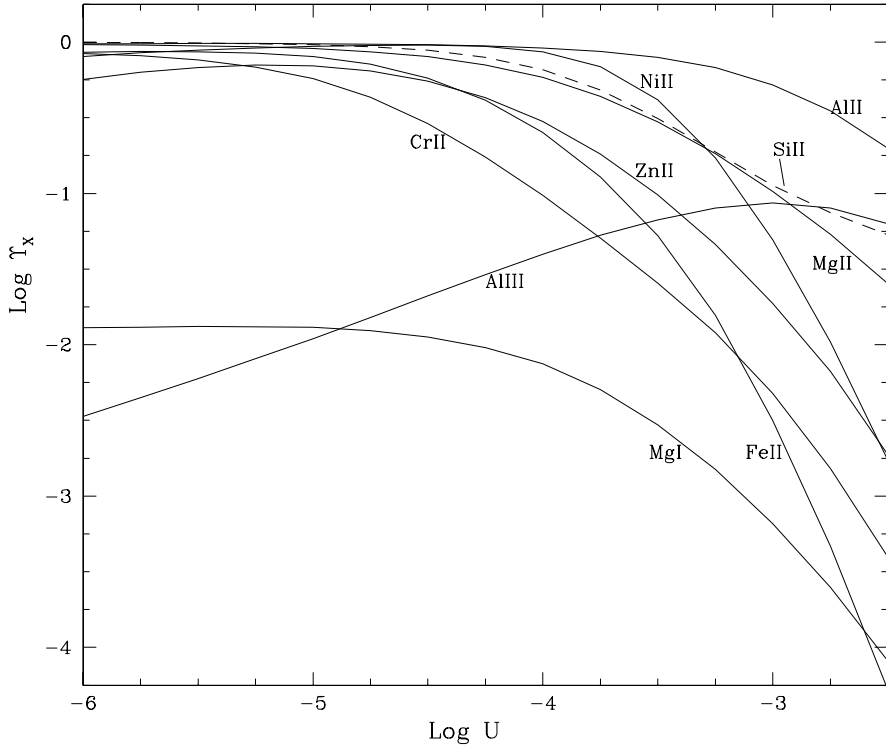


Figure 1: Fractional ionizations $\log \Upsilon_X$ vs. the ionization parameter $\log U$ in case of the Haardt-Madau [28] metagalactic UV background at $z = 3$ and metallicity $Z = 0.1Z_\odot$. Similarity of the line profiles of a pair of ions ‘a’ and ‘b’ requires the fractional ionization ratio Υ_a/Υ_b to be constant for different U

metagalactic spectrum at $z = 3$ presented in [28] ($n_{\text{ph}} \simeq 2 \times 10^{-5} \text{ cm}^{-3}$). Then fractional ionizations $\Upsilon_{a,i} = n_{a,i}/n_a$ (with n_a being the local number density of element ‘a’ and $n_{a,i}$ the density of ions in the i th ionization state) of different elements can be calculated as functions of U using the photoionization code CLOUDY [29].

Figure 1 shows these results for a metallicity $Z = 0.1Z_\odot$ (typical for the QSO metal absorbers) and for the elements involved in the MM analysis in [2]. Similar profiles for different ions can only be observed when the ratios $\Upsilon_{a,i}/\Upsilon_{b,j}$ are constant, i.e., the curves in Fig. 1 are parallel. This condition is realized for Mg I, Mg II, Al II, Si II, Fe II, Ni II, and Zn II in the

range $\log U < -4.2$, i.e., for the most dense volumes of the cloud. Such dense clumps (filaments) have, however, a negligible filling factor since their sizes are small, and, thus, the most of the diffuse cloud is filled up by a rarefied, low density gas characterized by higher values of $\log U$. In the range $\log U > -4$, the diversity of the Υ_X values is considerable and one may expect to observe nonsimilar profiles of the above mentioned ions. Under these circumstances, in order to be more secure the MM method should work with homogeneous samples of ions which have undoubtedly the same volume distribution like, e.g., Fe II lines.

Note that Al III is obviously not a good candidate for MM calculations since the shape of the $\Upsilon_{\text{Al III}}$ curve clearly differs from the others. The fact that no additional scatter in $\Delta\alpha/\alpha$ for systems containing Al III was found in [2] may imply that the available spectral resolution is not high enough to obtain the true profiles of the metal lines.

To conclude this section we comment on the accuracy $\sigma_{\Delta\alpha/\alpha}$ which can be in principle achieved from the up-to-date QSO observations. Using the method of error propagation, one finds from (10) the relative error of ω_z :

$$\delta_{\omega_z} \equiv \sigma_{\omega_z}/\omega_z = 2|Q|\sigma_{\Delta\alpha/\alpha}. \quad (12)$$

Here $Q = q/\omega_0$ is the dimensionless sensitivity coefficient.

For the lines listed in Table 2 in [2], the Q values are ranging from -0.027 (Cr II $\lambda 2066$ Å) to 0.050 (Zn II $\lambda 2026$ Å), however, for the most frequently used transitions in the MM calculations (Table 1 in [2]), this range is narrower: $Q(\text{Mg II } \lambda 2803$ Å) = 0.0034 , and $Q(\text{Fe II } \lambda 2600$ Å) = 0.035 . These numbers show that the error of the sample mean $\sigma_{\langle\Delta\alpha/\alpha\rangle} = 1.2 \times 10^{-6}$ found in [2] requires the relative error $\langle\delta_{\omega_z}\rangle \simeq 8.6 \times 10^{-9} - 8.4 \times 10^{-8}$, meaning that the sample mean wavelength accuracy should be $\langle\sigma_\lambda\rangle \simeq 2 \times 10^{-5} - 2 \times 10^{-4}$ Å at 2000 Å ($\sigma_\lambda = \lambda \delta_{\omega_z}$), which is equal to the radial velocity accuracy of $\Delta v \simeq 2.5 - 25$ m s $^{-1}$ ($\Delta v = c \delta_{\omega_z}$). Even if the individual measurement is an order of magnitude less accurate as compared to the sample mean, the uncertainty of $\Delta v \simeq 25 - 250$ m s $^{-1}$ seems to be hardly realized for all systems collected in [2]. Namely, the thermal shifts of order 300 m s $^{-1}$ are expected if temperature changes on 0.5 K between the science and calibration spectra exposures [23].

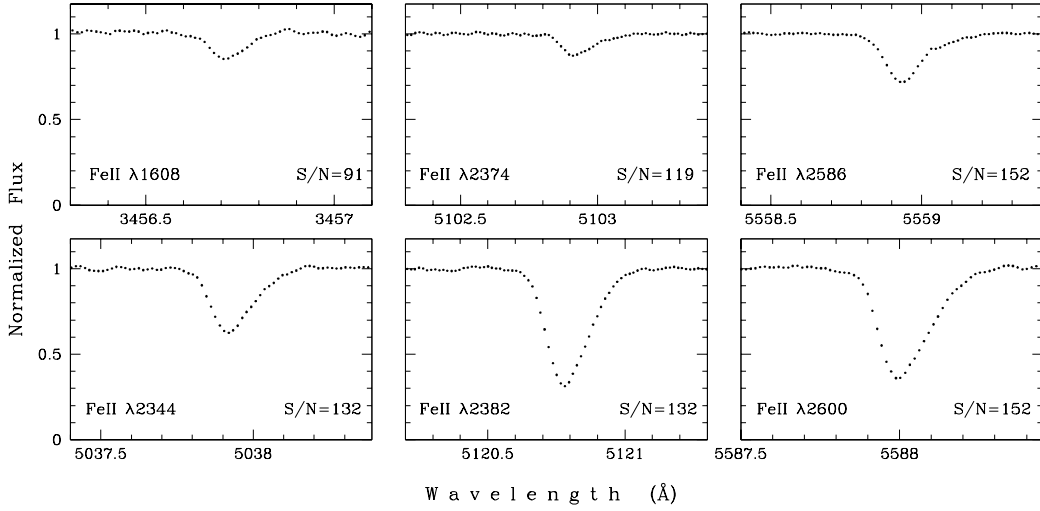


Figure 2: Fe II lines associated with the $z = 1.149$ absorption system toward the quasar HE 0515–4414 (normalized intensities are shown by dots). The mean signal-to-noise (S/N) ratios per resolution element are indicated

2.3 The regression MM method

The standard MM method based on the multiple velocity component Voigt profile fit to the complex spectra when $\Delta\alpha/\alpha$ is treated as an additional free parameter [2] can be easily modified to be free from the uncertainties mentioned in the previous section. By its very nature, the MM method is similar to that developed in [19] for the $\Delta\mu/\mu$ calculations. So, by analogy, we can re-write (10) in the linear approximation ($|\Delta\alpha/\alpha| \ll 1$) in the form

$$z_i = z_0 + \kappa_\alpha Q_i , \quad (13)$$

where the slope parameter κ_α is given by

$$\kappa_\alpha = 2(1 + z_0) \frac{\Delta\alpha^*}{\alpha} . \quad (14)$$

Here $\Delta\alpha^*/\alpha = -\Delta\alpha/\alpha$.

If $\Delta\alpha/\alpha$ is not zero, there should be a correlation between z_i ($= \lambda_{c,i}/\lambda_{0,i} - 1$) and Q_i , and the regression parameters z_0 and κ_α can be estimated from the measured centers of the isolated metal lines.

Table 1: Fe II lines at $z = 1.149$ toward the quasar HE 0515–4414 and sensitivity coefficients Q

λ_0^a , Å	f	λ_c , Å	W_λ , mÅ	z	Q
1608.45085(8)	0.0580 ^b	3456.7176(46)	7.8(1.8)	1.1490975(28)	-0.0193(48)
2344.2130(1)	0.1140 ^b	5037.9398(23)	27.5(1.6)	1.1490964(10)	0.0294(35)
2374.4603(1)	0.0313 ^b	5102.9319(79)	8.4(1.5)	1.1490913(33)	0.0389(35)
2382.7642(1)	0.3006 ^c	5120.8015(22)	61.0(1.9)	1.1491012(9)	0.0357(36)
2586.6496(1)	0.0684 ^d	5558.9439(29)	20.1(1.4)	1.1490904(11)	0.0393(39)
2600.1725(1)	0.2239 ^c	5588.0269(21)	59.1(2.0)	1.1490985(8)	0.0353(39)

^aVacuum rest wavelengths are taken from [2].

REFERENCES: ^bWelty et al. [33]; ^cMorton [34]; ^dCardelli & Savage [35].

For instance, Fe II lines listed in Table 2 in [2], for which the Q values are ranging in the broad interval between -0.019 and 0.035, may be suitable for such calculations. Equation (13) shows that the broader the interval of Q -values, the higher the accuracy of the slope parameter κ_α (see, e.g., [30] where the errors of the linear regression are calculated).

It is also an advantage that Fe II lines arise mainly in low ionized regions, where their thermal width is the smallest among other elements (Mg, Al, Si) proposed for the MM method (we do not consider Cr II, Ni II, and Zn II as appropriate for the MM analysis because they are rare in QSO spectra and, when observed, are usually very weak) since the narrow lines allow to measure the transition energies with highest accuracy. Below we consider an example of such Fe II sample.

Figure 2 shows isolated and unsaturated Fe II lines from the metal system at $z = 1.149$ toward the bright quasar HE 0515–4414. The spectra of this quasar were obtained with the UV-Visual Echelle Spectrograph (UVES) installed at the VLT/Kueyen telescope. The VLT/UVES data have a very high signal-to-noise ratio ($S/N \simeq 90 - 150$ per resolution element) and a high resolution power of $\lambda/\Delta\lambda \simeq 55\,000$ ($FWHM \simeq 5.5 \text{ km s}^{-1}$). The absorption

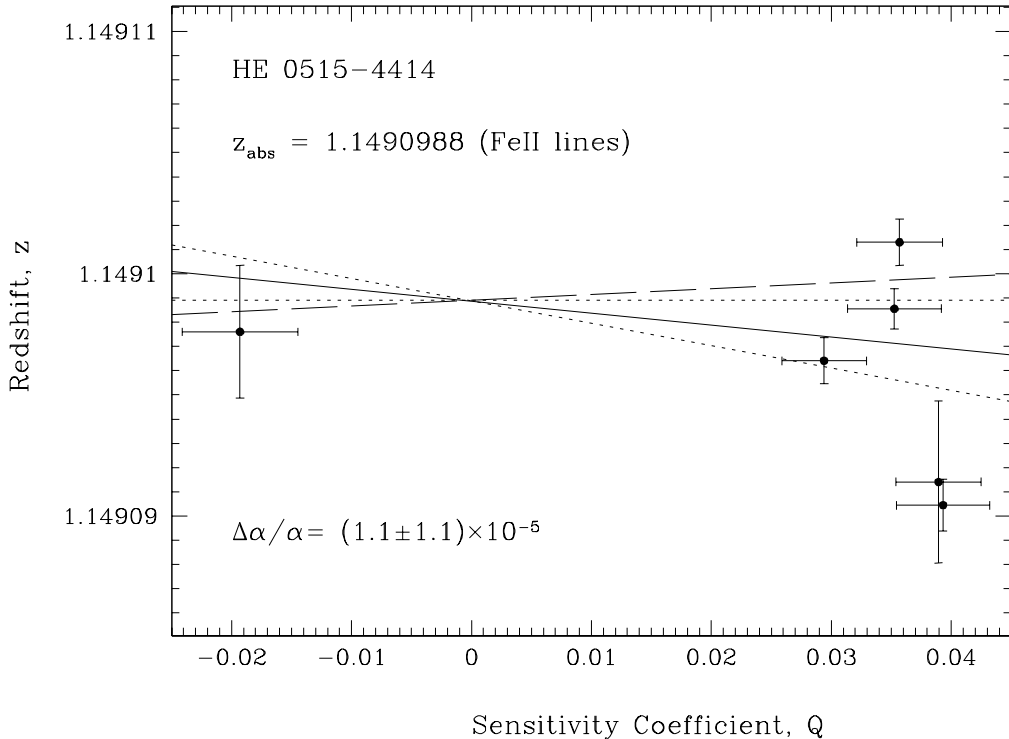


Figure 3: Relation between the redshifts z_i calculated for individual Fe II lines listed in Table 1 and their sensitivity coefficients Q_i . The solid line is the linear regression $z_i = z_0 + \kappa_\alpha Q_i$. The dotted lines representing the 1σ deviations from the optimal slope demonstrate that $\Delta\alpha/\alpha = 0$ at the level $\sim 2 \times 10^{-5}$. The dashed line is drawn for $\Delta\alpha/\alpha = -5.4 \times 10^{-6}$ found in the MM analysis in [2]

systems from this data were analyzed in [27] and [31, 32].

We used (4)-(8) to estimate the rest-frame equivalent widths W_λ , the line centers λ_c , and their errors which are listed in Table 1. In this table, column (2) presents the oscillator strengths for absorption. The sensitivity coefficients Q_i and their errors σ_{Q_i} are calculated from the values q_i , σ_{q_i} , and $\omega_{0,i}$ listed in Table 2 in [2].

Our result of the linear regression analysis is shown in Fig. 3 by the solid line, while two dotted lines correspond to the 1σ deviations of the slope parameter κ_α . We find $z_0 = 1.1490988 \pm 0.0000016$ and $\Delta\alpha/\alpha = (1.1 \pm 1.1) \times 10^{-5}$ (1σ). The uncertainties of the z_0 and $\Delta\alpha/\alpha$ values are calculated through statistical Monte Carlo simulations assuming that the deviations in the z_i and Q_i values are equally likely in the intervals $[z_i - \sigma_{z_i}, z_i + \sigma_{z_i}]$ and $[Q_i - \sigma_{Q_i}, Q_i + \sigma_{Q_i}]$. The result obtained shows that $\Delta\alpha/\alpha = 0$ within the 1σ interval. For comparison, the linear regression for $\Delta\alpha/\alpha = -5.4 \times 10^{-6}$ based on the inhomogeneous sample containing 127 absorption systems [2] is shown by the dashed line in Fig. 3. Although the sign of $\Delta\alpha/\alpha$ is opposite, the value of $\Delta\alpha/\alpha = -5.4 \times 10^{-6}$ is consistent with our data within the 2σ interval. The accuracy of the regression MM analysis may be increased if a few homogeneous samples are combined. The regression analysis is easily generalized for this case (see, e.g., [36]).

3 Constraints on the proton-to-electron mass ratio

The proton-to-electron mass ratio μ can be estimated from high redshift molecular hydrogen systems. With some modifications, such measurements were performed for the $z = 2.811$ H₂-bearing cloud toward the quasar PKS 0528–250 in [19] and [37] setting the limit of $|\Delta\mu/\mu| < 1.8 \times 10^{-4}$ (1σ). Later on higher resolution spectra of this QSO obtained with the VLT/UVES [38] revealed that the H₂ profiles at $z = 2.811$ are complex and consist of at least two subcomponents with $\Delta v \simeq 10$ km s⁻¹. Lines arising from the low rotational levels with $J = 0$ and $J = 1$ show a red-side asymmetry – contrary to those arising from $J = 2$ and $J = 3$ where a blue-side asymmetry is clearly seen. This complexity makes impossible higher accuracy measurements of $\Delta\mu/\mu$ in this system. Again, as in the case with the $\Delta\alpha/\alpha$ estimations, one needs a single component narrow H₂ absorption-line system to restrict the

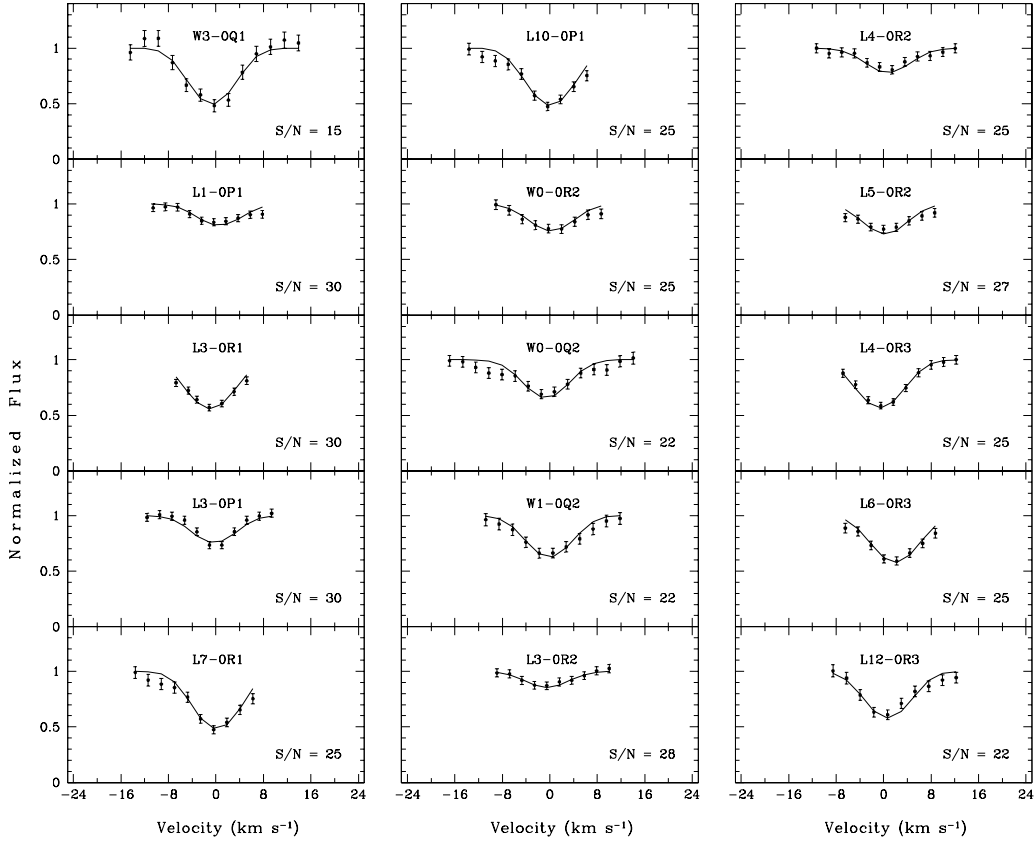


Figure 4: H_2 absorption features identified at $z = 3.025$ toward the quasar Q 0347–3819 (normalized intensities are shown by dots with 1σ error bars). The zero radial velocity is fixed at $z_{\text{H}_2} = 3.024895$. Smooth curves are the synthetic H_2 profiles found by the least-squares procedure. The mean S/N values per resolution element are indicated

observed wavelengths within the uncertainty interval of a few mÅ.

Such system has been found at $z = 3.025$ toward the quasar Q0347–3819 [39]. The absorption spectrum of this QSO was obtained with $FWHM \simeq 7 \text{ km s}^{-1}$ and $S/N \sim 15 - 30$ per resolution element at the VLT/UVES. 15 unblended H_2 lines (selected from ~ 80 identified H_2 transitions) which provide the most accurate line center measurements are shown in Fig. 4.

For a given H_2 line, the number of pixels involved in the analysis corresponds to the number of points in the line profile shown in Fig. 4. To measure the line centers we used a method that matches the observed profiles with the synthesized ones to estimate a set of model parameters (for details, see [23]). The results obtained are presented in Table 2. The measured individual z values and their standard deviations are listed in column (5). Using these redshifts we can constrain possible changes of μ .

The rest-frame wavelengths, $\lambda_{0,i}$, of different electronic-vibrational-rotational transitions of H_2 depend in a different way on the reduced mass of the molecule. The sensitivity of $\lambda_{0,i}$ to variation of μ is given by the sensitivity coefficient \mathcal{K}_i defined as [19]:

$$\mathcal{K}_i = \frac{\mu}{\lambda_{0,i}} \frac{d\lambda_{0,i}}{d\mu}. \quad (15)$$

Following the procedure described in [37] we calculate the coefficients \mathcal{K}_i listed in column (6) of Table 2. Their errors are obtained from coefficients Y_{mn} (presented in Table 1 in [37]) using the method of error propagation (Y_{mn} values are considered to be accurate to k decimal places and their rounding errors are set to 0.5×10^{-k}).

In linear approximation, (15) can be re-written in the form

$$\frac{\lambda_{i,z}/\lambda_{j,z}}{\lambda_{i,0}/\lambda_{j,0}} = 1 + (\mathcal{K}_i - \bar{\mathcal{K}}) \Delta\mu/\mu \quad (16)$$

or

$$z_i = z_0 + \kappa_\mu (\mathcal{K}_i - \bar{\mathcal{K}}), \quad (17)$$

where $\lambda_{i,z}$ and $\lambda_{j,z}$ are the line centers measured in a quasar spectrum, and

$$\kappa_\mu = (1 + z_0) \frac{\Delta\mu}{\mu}, \quad (18)$$

with z_0 and $\bar{\mathcal{K}}$ being the mean redshift and the mean sensitivity coefficient, respectively.

Table 2: H_2 lines at $z = 3.025$ toward Q 0347–3819 and sensitivity coefficients \mathcal{K}

J	Line	$\lambda_0^a, \text{\AA}$	$\lambda_c, \text{\AA}$	z	\mathcal{K}
1 ...	W3-0Q	947.4218(5)	3813.2653(41)	3.024887(5)	0.0217427(8)
	L1-0P	1094.0522(51)	4403.4575(77)	3.02491(2)	-0.0023282(1)
	L3-0R	1063.4603(1)	4280.3051(30)	3.024885(3)	0.0112526(4)
	L3-0P	1064.6056(5)	4284.9249(33)	3.024894(4)	0.0102682(4)
	L7-0R	1013.4412(20)	4078.9785(25)	3.024898(9)	0.03050(1)
	L10-0P	982.8340(6)	3955.8049(51)	3.024896(6)	0.04054(6)
2 ...	W0-0R	1009.0233(7)	4061.2194(61)	3.024901(7)	-0.0050567(7)
	W0-0Q	1010.9380(1)	4068.9088(53)	3.024885(6)	-0.0068461(2)
	W1-0Q	987.9744(20)	3976.4943(49)	3.02490(1)	0.0039207(2)
	L3-0R	1064.9935(9)	4286.4755(98)	3.02488(1)	0.0097740(5)
	L4-0R	1051.4981(4)	4232.1793(85)	3.024904(8)	0.015220(1)
	L5-0R	1038.6855(32)	4180.6048(70)	3.02490(1)	0.020209(3)
3 ...	L4-0R	1053.9770(11)	4242.1419(28)	3.024890(5)	0.012837(2)
	L6-0R	1028.9832(16)	4141.5758(31)	3.024921(7)	0.022332(7)
	L12-0R	967.6752(21)	3894.7974(39)	3.02490(1)	0.0440(2)

^aListed wavelengths are from [40, 41].

The linear regression (17) calculated for the complete sample of the H₂ lines from Table 2 provides $(\Delta\mu/\mu)_{J=1+2+3} = (5.0 \pm 3.2) \times 10^{-5}$. However, if we consider H₂ transitions from individual J levels, then the weighted mean redshifts reveal *a gradual shift in the radial velocity* for features arising from progressively higher rotational levels : $z(J=1) = 3.024890(2)$, $z(J=2) = 3.024895(3)$, and $z(J=3) = 3.024904(4)$. The H₂ lines with changing profiles and small velocity shifts as J increases were also observed in our Galaxy in the direction of ζ Ori A. At present these H₂ lines are interpreted as being formed in *different zones* of a postshock gas [42].

Although the $z(J=1)$ and $z(J=2)$ values are consistent within 1σ intervals, the difference between $z(J=1)$ and $z(J=3)$ is essential and equals $1.0 \pm 0.3 \text{ km s}^{-1}$. This small change in the radial velocity with increasing J may mimic a shift in $\Delta\mu/\mu$. If we exclude from the regression analysis the rotational levels with $J = 3$, then $(\Delta\mu/\mu)_{J=1+2} = (2.1 \pm 3.6) \times 10^{-5}$. The use of lines arising from the same rotational levels would be more reasonable to estimate $\Delta\mu/\mu$, but in our case the sample size is rather small and we have to combine the $J = 1$ and $J = 2$ levels to increase statistics. The linear regression is shown by the solid line in Fig. 5 while two dashed lines correspond to the 1σ deviations of the slope parameter κ_μ .

Thus, the 1σ confidence interval to $\Delta\mu/\mu$ is $-1.5 \times 10^{-5} < \Delta\mu/\mu < 5.7 \times 10^{-5}$. For a cosmological model with $\Omega_M = 0.3$, $\Omega_\Lambda = 0.7$, and $H_0 = 72 \text{ km s}^{-1} \text{ Mpc}^{-1}$, the look-back time for $z = 3.025$ is 11.2 Gyr [43]. This leads to the restriction $|\dot{\mu}/\mu| < 5 \times 10^{-15} \text{ yr}^{-1}$ on the variation rate of μ .

4 Conclusions and future prospects

We have considered modern experimental investigations of the hypothetical variations of the fundamental physical constants from absorption-line spectra of distant quasars. The subject was limited to the properties of the two dimensionless quantities – the fine-structure constant α and the proton-to-electron mass ratio μ . Our main conclusions are as follows:

- The accuracy $\sigma_{\langle\Delta\alpha/\alpha\rangle} = 1.2 \times 10^{-6}$ claimed in [2] is an order of magnitude higher compared to what can be provided by the wavelength measurements of isolated and unsaturated QSO absorption lines. Taking into account all shortcomings of the MM method as it was used in [2], the quoted value of $\sigma_{\langle\Delta\alpha/\alpha\rangle}$ is likely to be overestimated.

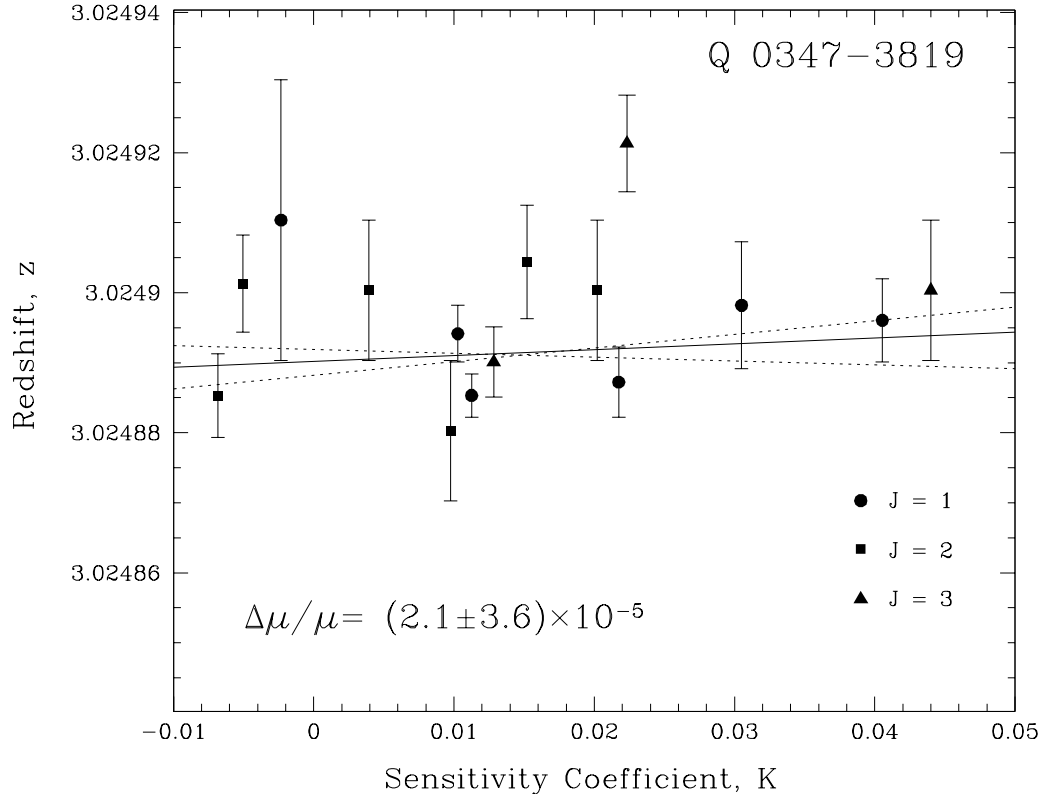


Figure 5: Relation between the redshift values z_i calculated for individual H_2 lines shown in Fig. 4 and their sensitivity coefficients \mathcal{K}_i . The solid line is the linear regression $z_i = z_0 + \kappa_\mu(\mathcal{K}_i - \bar{\mathcal{K}})$. The dotted lines representing the 1σ deviations from the optimal slope κ_μ demonstrate that $\Delta\mu/\mu = 0$ at the level $\sim 5 \times 10^{-5}$.

- A modification of the MM method (regression MM method) which makes it more reliable is presented. This modified MM method applied to the homogeneous sample of the isolated and unsaturated Fe II lines yields $\Delta\alpha/\alpha = (1.1 \pm 1.1) \times 10^{-5}$. The uncertainty of this value is in agreement with the available accuracy of the wavelength measurements.
- If the fine-structure constant varies at the level of $\Delta\alpha/\alpha = (-5.4 \pm 1.2) \times 10^{-6}$ [2], then the link between α_z/α and the proton-to-electron mass ratio μ_z/μ expected within the grand unification theories (e.g., [18]) leads to the shift $\Delta\mu/\mu \sim -2 \times 10^{-4}$. This prediction is *not confirmed*. The variability of μ is constrained by the values $-1.5 \times 10^{-5} < \Delta\mu/\mu < 5.7 \times 10^{-5}$ at redshift $z = 3.025$ [23].

As stated above, the accuracy of $\sigma_\lambda \sim 0.2$ mÅ is required to achieve a level higher than 10^{-5} in the $\Delta\alpha/\alpha$ measurements. This accuracy is ~ 10 times higher than available at modern giant telescopes. In 2003, a new High Accuracy Radial velocity Planet Searcher (HARPS) spectrograph [44] started to operate at the 3.6 m telescope (ESO, La Silla, Chile). Observations with HARPS may in principle provide this desirable accuracy. With a resolving power of $\lambda/\Delta\lambda = 120\,000$ and a projection of the fiber over 4 pixels, one HARPS pixel corresponds to $\simeq 600$ m s $^{-1}$. For an isolated and unsaturated absorption line, the line center may be measured with an accuracy of about 1/20 of the pixel size (~ 30 m s $^{-1}$). This corresponds to $\sigma_\lambda = 0.4$ mÅ at 4000 Å. If isotopic and hyperfine structure systematics as well as the others discussed in [2] are known, then we may hope to reach a level of $\sim 10^{-6}$ in future astronomical measurements of $\Delta\alpha/\alpha$.

Acknowledgments

This work is supported in part by the RFBR grant No. 03-02-17522. I thank the organizing committee for providing me with the opportunity to attend. I especially thank Sandro D’Odorico, Luca Pasquini, Dieter Reimers, and Robert Baade for helpful discussions.

References

- [1] V. A. Dzuba, V. V. Flambaum, J. K. Webb: Phys. Rev. Lett. **82**, 888 (1999)
- [2] M. T. Murphy, J. K. Webb, V. V. Flambaum: Mon. Not. R. Astron. Soc., in press, astro-ph/0306483 (2003)
- [3] P. J. Mohr, B. N. Tailor: Rev. Mod. Phys. **72**, 351 (2000)
- [4] E. A. Milne: Proc. R. Soc. A **158**, 324 (1937)
- [5] P. A. M. Dirac: Nature **139**, 323 (1937)
- [6] J. Uzan: Rev. Mod. Phys. **75**, 403 (2003)
- [7] A. Chodos, S. Detweiler: Phys. Rev. D **21**, 2167 (1980)
- [8] W. J. Marciano: Phys. Rev. Lett. **52**, 489 (1984)
- [9] Y. S. Wu, Z. Wang: Phys. Rev. Lett. **57**, 1978 (1986)
- [10] P. D. B. Collins, A. Martin, E. J. Squires: *Particle Physics and Cosmology* (Wiley, New York 1989)
- [11] J. D. Barrow, J. Maguejo, H. B. Sandvik: Phys. Rev. D **66**, 3515 (2002)
- [12] J. P. Mbelek, M. Lachièze-Rey: Astron. Astrophys. **397**, 803 (2003)
- [13] J. N. Bahcall, C. L. Steinhardt, D. Schlegel: Astrophys. J., in press, astro-ph/0301507 (2003)
- [14] J. N. Bahcall, W. L. W. Sargent, M. Schmidt: Astrophys. J. **149**, L11 (1967)
- [15] D. A. Varshalovich, A. Y. Potekhin: Astron. Lett. **20**, 771 (1994)
- [16] D. A. Varshalovich, A. Y. Potekhin, A. V. Ivanchik: ‘Testing cosmological variability of fundamental constants’. In: *X-ray and Inner-Shell Processes*. ed. by R. W. Danford, D. S. Gemmel, E. P. Kauter, B. Kraesig, S. H. Southworth, L. Yong (AIP, Melville 2000) pp. 503–511

- [17] M. T. Murphy, J. K. Webb, V. V. Flambaum, J. X. Prochaska, A. M. Wolfe: Mon. Not. R. Astron. Soc. **327**, 1237 (2001)
- [18] P. Langacker, G. Sergè, M. J. Strassler: Phys. Lett. B **528**, 121 (2002)
- [19] D. A. Varshalovich, S. A. Levshakov: JETP Lett. **58**, 237 (1993)
- [20] J. N. Bahcall, M. Schmidt: Phys. Rev. Lett. **19**, 1294 (1967)
- [21] S. A. Levshakov: Mon. Not. R. Astron. Soc. **269**, 339 (1994)
- [22] R. C. Bohlin, J. K. Hill, E. B. Jenkins, B. D. Savage, T. P. Snow, L. Spitzer, D. G. York: Astrophys. J. Suppl. Ser. **51**, 277 (1983)
- [23] S. A. Levshakov, M. Dessauges-Zavadsky, S. D'Odorico, P. Molaro: Mon. Not. R. Astron. Soc. **333**, 373 (2002)
- [24] L. Lu, W. L. W. Sargent, T. A. Barlow, C. W. Churchill, S. S. Vogt: Astrophys. J. Suppl. Ser. **107**, 475 (1996)
- [25] S. A. Levshakov, F. Takahara, I. I. Agafonova: Astrophys. J. **517**, 609 (1999)
- [26] S. A. Levshakov, I. I. Agafonova, W. H. Kegel: Astron. Astrophys. **360**, 833 (2000)
- [27] D. Reimers, R. Baade, R. Quast, S. A. Levshakov: Astron. Astrophys., in press, astro-ph/0308432 (2003)
- [28] F. Haardt, P. Madau: Astrophys. J., **461**, 20 (1996)
- [29] G. Ferland: *A Brief Introduction to Cloudy* (Internal Rep., Lexington, Univ. Kentucky, 1997)
- [30] W. H. Press, S. A. Teukolsky, W. T. Vetterling, B. P. Flannery: *Numerical Recipes in C* (Cambridge Univ. Press, Cambridge 1992)
- [31] R. Quast, R. Baade, D. Reimers: Astron. Astrophys. **386**, 796 (2002)
- [32] S. A. Levshakov, I. I. Agafonova, D. Reimers, R. Baade: Astron. Astrophys. **404**, 449 (2003)

- [33] D. E. Welty, L. M. Hobbs, J. T. Lauroesch, et al.: *Astrophys. J. Suppl. Ser.* **124**, 465 (1999)
- [34] D. C. Morton: *Astrophys. J. Suppl. Ser.* **77**, 119 (1991)
- [35] J. Cardelli, B. D. Savage: *Astrophys. J.* **452**, 275 (1995)
- [36] A. V. Ivanchik, E. Rodriguez, P. Petitjean, D. A. Varshalovich: *Astron. Lett.* **28**, 423 (2002)
- [37] A. Y. Potekhin, A. V. Ivanchik, D. A. Varshalovich, K. M. Lanzetta, J. A. Baldwin, G. M. Williger, R. F. Carswell: *Astrophys. J.* **505**, 523 (1998)
- [38] S. A. Levshakov, M. Centurión, W. H. Kegel, P. Molaro: in preparation (2003)
- [39] S. A. Levshakov, M. Dessauges-Zavadsky, S. D'Odorico, P. Molaro: *Astrophys. J.* **565**, 696 (2002)
- [40] H. Abgrall, E. Roueff, F. Launay, J.-Y. Roncin, J.-L. Subtil: *Astron. Astrophys. Suppl. Ser.* **101**, 273 (1993)
- [41] H. Abgrall, E. Roueff, F. Launay, J.-Y. Roncin, J.-L. Subtil: *Astron. Astrophys. Suppl. Ser.* **101**, 323 (1993)
- [42] E. B. Jenkins, A. Peimbert: *Astrophys. J.* **477**, 265 (1997)
- [43] S. M. Carroll, W. H. Press, E. L. Turner: *Ann. Rev. Astron. Astrophys.* **30**, 499 (1992)
- [44] F. Pepe, M. Mayor, G. Rupprecht et al.: *ESO Messenger* **110**, 9 (2002)